Supplementary Information for:

Global mapping of GalNAc-T isoform-specificities and O-glycosylation site-occupancy in a tissue-forming human cell line

Mathias I. Nielsen**, Noortje de Haan**, Weston Kightlinger, Zilu Ye, Sally Dabelsteen, Minyan Li, Michael C. Jewett, Ieva Bagdonaite, Sergey Y. Vakhrushev*, and Hans H. Wandall*

*To whom correspondence should be addressed. E-mail: hhw@sund.ku.dk and seva@sund.ku.dk

** Equally contributing authors.

This PDF file includes:

Supplementary Figures 1 to 4

Supplementary Figure 1

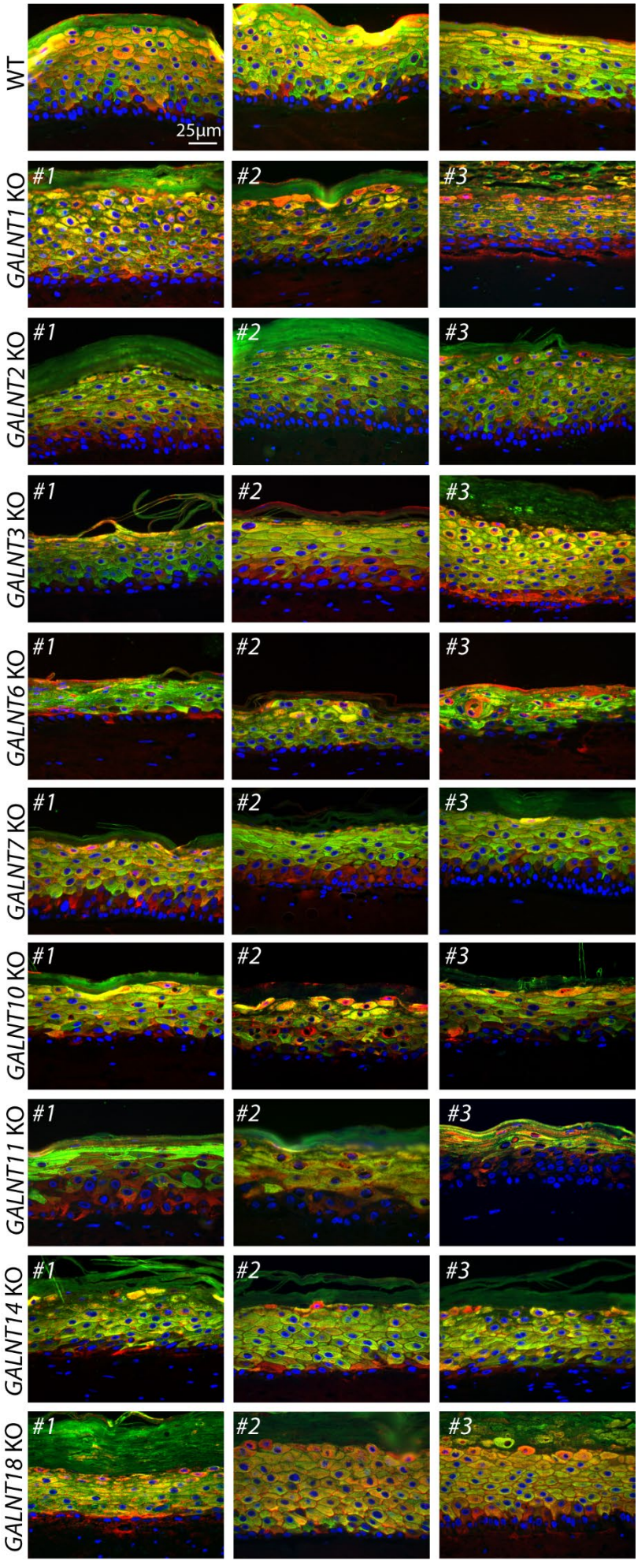

Supplementary Figure 1: Micrographs show sections of organotypic cultures (OCT) made with three different clones of *GALNT* KO tissues. At least three independent experiments were performed for each clone at different time points resulting in organotypic cultures with similar morphologies. Sections are stained with differentiation markers Keratin10 (green) and Involucrin (red). Nuclei labelled with DAPI (blue). Scalebar = 25µm.

Supplementary Figure 2

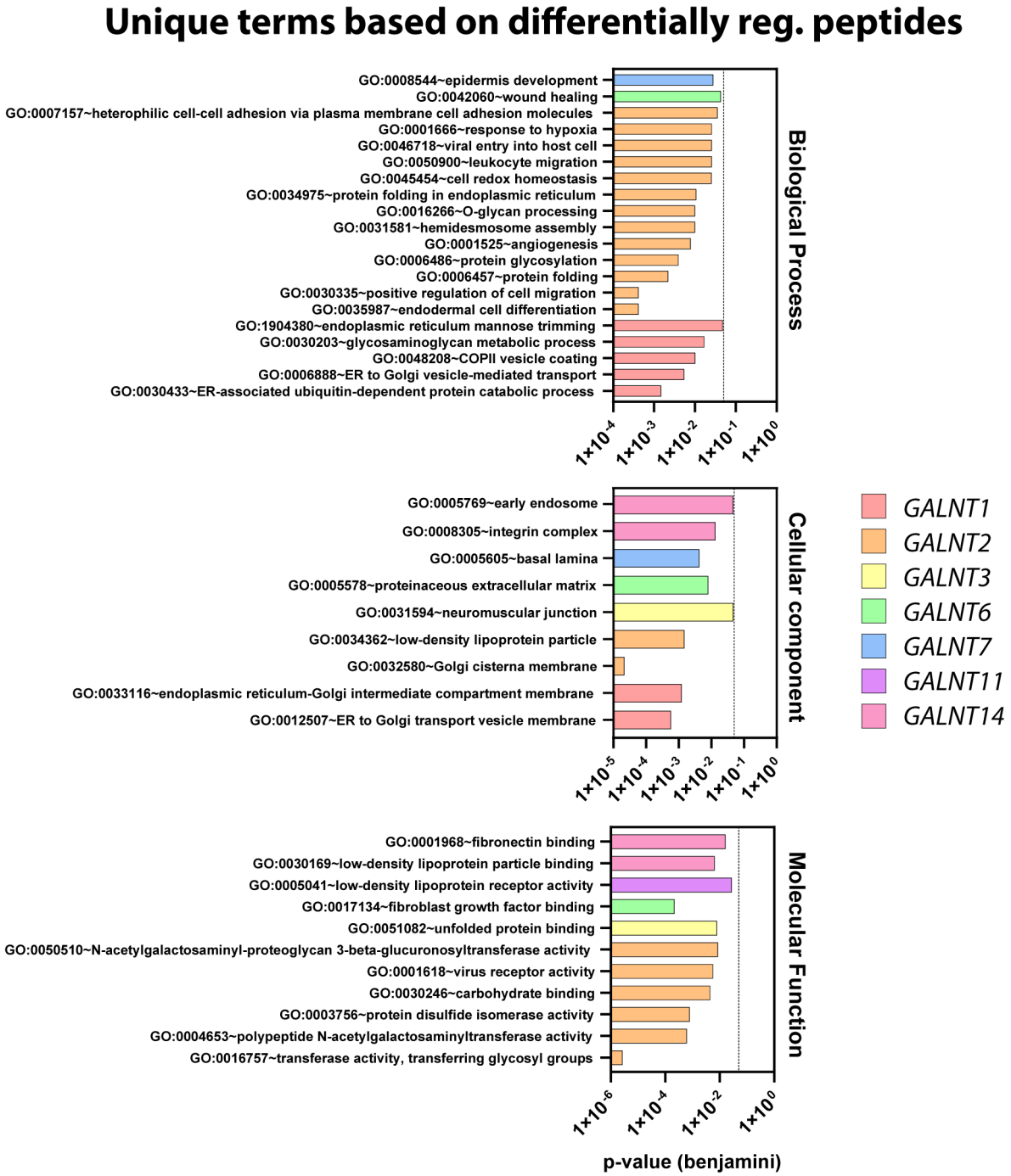

Supplementary Figure 2: Gene Ontology (GO)-term analysis of differentially glycosylated protein identifications (DAVID, q≤0.05, Benjamini adjusted). Each color represents differential GO terms unique to one of the *GALNT* differential datasets. Pvalue (Benjamini multiple comparison adjusted) of 0.05 is marked with a dashed line. Additional information can be found in Supplementary Figure 2 associated table below.

Supplementary Figure 2 associated table. Additional GO-term analysis information

GALNT	Category	Term	Count	Pvalue	Genes	Benjamini
T1	BP	GO:0030433~ER-associated ubiquitin-dependent protein catabolic process	6	5.34E-06	Q9UBV2, P11021, Q13438, P14625, Q9UKM7, O94905	0.001487
T1	BP	GO:0006888~ER to Golgi vesicle-mediated transport	7	5.85E-05	Q8NI22, P49257, Q5JRA6, Q15363, P49755, P15514, Q9Y4L1	0.005432
T1	BP	GO:0048208~COPII vesicle coating	5	0.000128	Q8NI22, P49257, Q15363, P49755, P15514	0.010158
T1	BP	GO:0030203~glycosaminoglycan metabolic process	4	0.000245	P35052, P18827, Q4G148, P98160	0.01703
T1	BP	GO:1904380~endoplasmic reticulum mannose trimming	3	0.000776	Q9UBV2, Q13438, Q9UKM7	0.048026
T1	CC	GO:0012507~ER to Golgi transport vesicle membrane	5	5.85E-05	Q8NI22, P49257, Q15363, P49755, P15514	0.000581
T1	CC	GO:0033116~endoplasmic reticulum-Golgi intermediate compartment membrane	5	0.000132	Q8NI22, P49257, Q15363, P49755, P15514	0.001233
T2	BP	GO:0035987~endodermal cell differentiation	6	2.03E-06	P08648, Q13751, Q16787, P50281, P08572, P02751	0.000419
T2	BP	GO:0030335~positive regulation of cell migration	11	2.06E-06	P08648, Q13753, P00749, P11021, P50281, O00592, P13726, P43121, P21709, P07996, O00622	0.000419
T2	BP	GO:0006457~protein folding	10	1.33E-05	P11142, Q8NBS9, Q9BS26, Q96KC8, P14625, P13667, P27824, Q14696, P14314, P30101	0.002199
T2	BP	GO:0006486~protein glycosylation	8	3.21E-05	Q96FL9, Q9HCN8, O60513, Q93063, O60512, Q9H6U8, Q8NCL4, Q10471	0.003976
T2	BP	GO:0001525~angiogenesis	10	7.16E-05	P08648, P29279, P50281, P43121, O60462, P08572, P21709, P35354, P78504, P02751	0.007881
T2	BP	GO:0031581~hemidesmosome assembly	4	0.000101	Q13753, Q13751, Q16787, Q9UMD9	0.010029
T2	BP	GO:0016266~O-glycan processing	6	0.000111	Q96FL9, Q14435, Q8NCL4, Q7Z7M9, Q8NBI6, Q10471	0.010029
T2	BP	GO:0034975~protein folding in endoplasmic reticulum	4	0.000131	P11021, P14625, P27824, P30101	0.010826
T2	BP	GO:0045454~cell redox homeostasis	6	0.000362	Q8NBS9, Q9BS26, P13667, Q9BQE4, P30101, P07237	0.025605
T2	BP	GO:0050900~leukocyte migration	7	0.000421	P08648, Q9Y624, O00592, P08195, P16070, P02751, P05026	0.025726
T2	BP	GO:0046718~viral entry into host cell	6	0.000432	P08648, Q9Y624, P01130, Q92692, Q14118, P18564	0.025726
T2	BP	GO:0001666~response to hypoxia	8	0.000441	P00749, P50281, P19021, P14625, Q92544, Q14571, P07996, P05026	0.025726
T2	BP	GO:0007157~heterophilic cell-cell adhesion via plasma membrane cell adhesion molecules	5	0.000653	Q9NT68, P08648, Q9P273, Q92692, Q9NQS3	0.035966
T2	CC	GO:0032580~Golgi cisterna membrane	8	2.1E-06	O60513, Q86X52, Q14435, O60512, Q8IZ52, O00461, Q9P2E5, Q10471	2.18E-05
T2	CC	GO:0034362~low-density lipoprotein particle	4	0.000158	P01130, Q86X29, Q92673, Q9BQE4	0.001485
T2	MF	GO:0016757~transferase activity, transferring glycosyl groups	9	2.21E-08	Q96FL9, O60513, Q93063, O60512, Q9H6U8, Q8NCL4, Q8N3Y3, Q8NBI6, Q10471	2.7E-06
T2	MF	GO:0004653~polypeptide N-acetylgalactosaminyltransferase activity	5	1.52E-05	Q96FL9, Q14435, Q8NCL4, Q7Z7M9, Q10471	0.00062
T2	MF	GO:0003756~protein disulfide isomerase activity	5	2.27E-05	Q8NBS9, Q9BS26, P13667, P30101, P07237	0.000792
T2	MF	GO:0030246~carbohydrate binding	9	0.000146	Q96FL9, Q14435, Q13438, Q8NCL4, Q7Z7M9, P27824, Q12907, Q9UBG0, Q10471	0.004467
T2	MF	GO:0001618~virus receptor activity	6	0.000211	P08648, Q9Y624, P01130, Q92692, Q14118, P18564	0.005711
T2	MF	GO:0050510~N-acetylgalactosaminyl-proteoglycan 3-beta-glucuronosyltransferase activity	3	0.000355	Q86X52, Q8IZ52, Q9P2E5	0.008661
T3	CC	GO:0031594~neuromuscular junction	3	0.005864	P05556, P05067, O75096	0.04728
T3	MF	GO:0051082~unfolded protein binding	5	0.000106	P30533, P11021, P14625, P27824, P50454	0.007944
T6	BP	GO:0042060~wound healing	5	0.000384	P18827, Q5JRA6, Q9NYQ6, P22223, P31431	0.043189
T6	CC	GO:0005578~proteinaceous extracellular matrix	7	0.000824	P35052, P23471, P19957, Q9UMD9, Q92896, Q16610, Q9NZU0	0.007984
T6	MF	GO:0017134~fibroblast growth factor binding	5	2.13E-06	P35052, Q14512, P06756, P22607, Q92896	0.000217
T7	BP	GO:0008544~epidermis development	4	0.000335	P22528, P12272, Q9UMD9, Q9UBC9	0.028037
T7	CC	GO:0005605~basal lamina	3	0.000253	O00468, P02751, P14543	0.004258
T11	MF	GO:0005041~low-density lipoprotein receptor activity	2	0.002309	P01130, Q07954	0.027704
T14	CC	GO:0008305~integrin complex	3	0.001085	P05556, P23229, P26006	0.013345
T14	CC	GO:0005769~early endosome	4	0.008093	Q5VW38, P01130, O14786, Q92673	0.047401
T14	MF	GO:0030169~low-density lipoprotein particle binding	3	0.000383	P01130, Q92673, P07996	0.006434
T14	MF	GO:0001968~fibronectin binding	3	0.00117	P05556, P07996, P26006	0.016374

Supplementary Figure 3

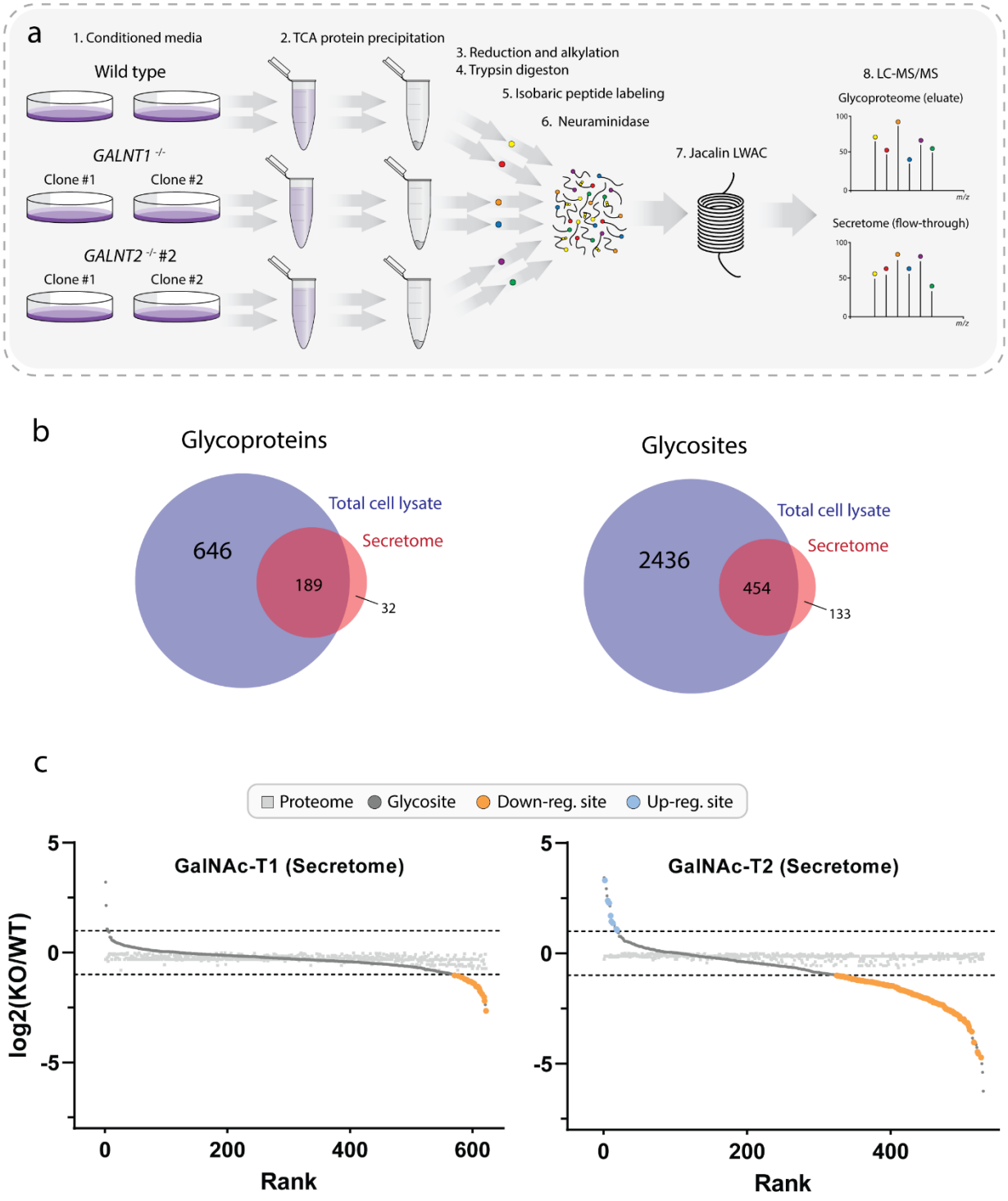

Supplementary Figure 3: Differential N/TERT-1 secretomes. **a)** Workflow summary for preparation on differential glycosecretomes. Conditioned media was harvested from N/TERT-1 WT and *GALNT1* and *-T2* knockout cells, and secreted proteins were isolated using trichloroacetic acid (TCA) precipitation. Secreted protein samples were then subjected to a similar glycoproteomic workflow as described in Figure 1A. **b)** Comparison of glycoproteins and glycosites identified in total cell lysate samples (blue) and secretome samples (red). **c)** Rank curve plot showing change in secretome glycopeptide (dark grey circles) abundances for *GALNT1* and *-T2* knockouts. Orange circles represent significantly down-regulated glycopeptides (p-value < 0.05 and log2 fold change < -1) and blue circles represent significantly up-regulated glycopeptides (p-value < 0.05 and log2 fold change >1). Sites from proteins with overall abundance change in the proteome (light grey squares) were removed. Source data are in Supplementary Data 2.

Supplementary Figure 4

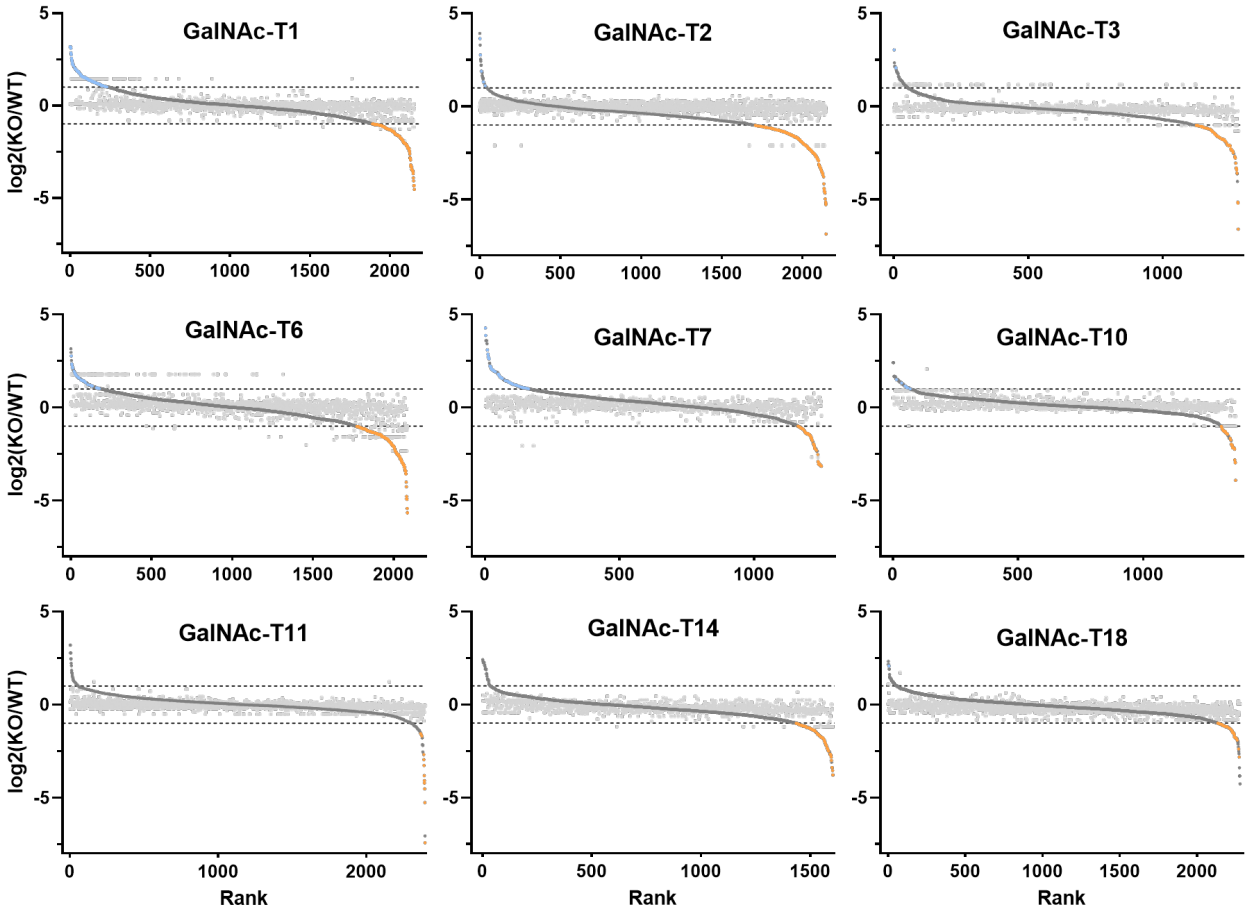

Supplementary Figure 4: Rank curve plot showing change in glycopeptide (dark grey circles) abundance for each of the 9 *GALNT* knockouts. Orange circles represent significantly down-regulated glycopeptides (*p*-value < 0.05 and log2 fold change < -1) and blue circles represent significantly up-regulated glycopeptides (*p*-value < 0.05 and log2 fold change >1). For each of the nine targeted *GALNT* genes, knockouts (n = 3 biologically independent samples) were compared in a multiplexed experiment with wild type material (n = 3 technically independent samples). A two-sided Student's t-test was used as a measure of statistical confidence and the *p*-values were adjusted for multiple testing, using an FDR of 5%. Source data are in Supplementary Data 2 and 4.